Renewable Energy xxx (xxxx) 121440

Contents lists available at ScienceDirect

Renewable Energy

journal homepage: www.elsevier.com/locate/renene

Comparative study of grass pyrolysis over regenerated catalysts: Tyre ash, zeolite, and nickel-supported ash and zeolite

Wojciech Jerzak *, Małgorzata Sieradzka, Mariusz Wądrzyk, Aneta Magdziarz

AGH University of Krakow, Mickiewicza 30, 30-059, Krakow, Poland

ARTICLE INFO

Keywords:
Tyre ash
Catalyst regeneration
Biomass
Pyrolysis
Zeolite
Coke

ABSTRACT

This paper presents investigations on catalytic and non-catalytic grass pyrolysis conducted at 500 °C using two reactor scales: a micro-scale reactor and a laboratory fixed-bed reactor. Four catalysts were employed in the catalytic pyrolysis process: car tyre ash, commercial zeolite mordenite-sodium, nickel supported on ash, and nickel supported on zeolite. The use of catalysts reduced the production of oxygenates and promoted the formation of gaseous compounds, with the most pronounced effect observed for nickel supported on zeolite. Catalytic pyrolysis produced chars with yields that were higher than those of the non-catalytic process. The coking behaviour of the spent catalysts was evaluated by analysing carbon content, with the highest content (3 wt% C) obtained for ash after the first cycle. In the second cycle, the deposited carbon content decreased for all catalysts. Furthermore, the employment of catalysts was shown to promote the production of hydrogen, methane, and other hydrocarbons in pyrolysis gas. The higher heating value of the pyrolysis gas was the highest at 21.1 MJ/m^3 when the ash catalyst was first used for pyrolysis. Reusing the pyrolysis catalysts slightly reduced the heating value of the gas to 20.3 MJ/m^3 over ash and 20.6 MJ/m^3 over zeolite.

1. Introduction

The use of renewable energy in the European Union (EU) in 2022 was 23 % of the total energy consumption, compared to 21.9 % in 2021, according to data announced by the European Environment Agency [1]. This increase was largely due to the development of solar energy. However, it notes that achieving the new 42.5 % target for 2030 will require a significant acceleration in the deployment of renewable energy sources compared to previous decades. Eurostat emphasised the dominance of solid biomass as a renewable energy source. The total biomass sources in the EU are approximately 1 billion tonnes of dry matter [2]. Over time, the EU has demonstrated an escalating trend in biomass procurement, encompassing both primary and secondary sources. Primary types of biomass include plant materials such as crops, wood and fruit and must be used in a sustainable way. Secondary sources of biomass are agricultural and forestry residues, fish and animal waste, industrial waste (np. beer brewing industry), paper mill sludge, and sewage. By taking action to use secondary biomass into fuel and energy production, the concepts of waste-to-energy (WTE) and circular economy (reduce, reuse, recycle and recover - 4R) are promoted [3].

Biochemical and thermochemical methods are pivotal processes used to convert biomass into renewable fuels, valuable chemicals, or energy [4]. Biochemical methods are more time-consuming than thermochemical methods [5]. Thermochemical conversion processes include combustion, gasification, pyrolysis, and hydrothermal liquefaction, each offering distinct advantages [6]. Pyrolysis, in particular, has attracted significant attention due to its broad applicability [7]. It involves the thermal cracking of organic substances in a controlled oxygen-deprived environment at moderate temperatures. This rapid and controlled degradation process makes thermochemical methods, such as pyrolysis, promising avenues for efficient biomass utilisation in the renewable energy sector [8]. One of the challenges related to the development of thermochemical biomass conversion technologies and their industrial use is the high energy input required for biomass conversions [9]. The heat of reaction required for the pyrolysis of biomass waste ranges from 0.9 to 2 MJ/kg [10]. To overcome this problem, catalysts should be used for pyrolysis [11]. Catalysts help to lower operating temperatures, enhance conversion efficiency, and improve selectivity towards valuable chemicals [12]. Despite the growing interest and research in catalyst utilisation, challenges remain due to the complex nature of biomass.

* Corresponding author.
E-mail address: wjerzak@agh.edu.pl (W. Jerzak).

https://doi.org/10.1016/j.renene.2024.121440
Received 31 May 2024; Received in revised form 7 August 2024; Accepted 20 September 2024
0960-1481/

Generally, there are two main approaches to the catalytic pyrolysis of biomass: in-situ and ex-situ methods [13]. In the in-situ method, biomass and catalysts are usually mixed in a single reactor, simplifying device investment, but risking poor heat transfer and catalyst deactivation due to limited contact between phases [14]. Studies in which catalysts were not mixed with biomass have also been reported [15]. On the contrary, ex-situ pyrolysis in a dual-bed reactor allows for better control over reaction conditions and selectivity to target products such as aromatics, although at a higher cost [16]. Various catalysts (zeolites, silica materials, activated carbons) have been explored to suit different pyrolysis systems and product demands [17]. Catalysts based on ash from coal, biomass, and other waste are gaining popularity and are increasingly used in pyrolysis processes. Ash, one of the main by-products of industry, is a significant priority for alternative applications beyond current landfill practices. One of the basic arguments for the use of ashes as catalysts is their relatively low cost [18]. In addition, ash has unique properties that increase the efficiency of biomass conversion. The catalytic properties of coal and biomass ashes used during pyrolysis have been reported many times. To improve their catalytic activity, the ashes are modified. Acid and alkali treated coal fly ash increases H_2 production during coal pyrolysis and improves carbon conversion [19]. The modification of the ash leads to a significant loss of $CaSO_4$, the formation of the new phases (e.g. iron fluoride when HF was used) and increases the specific surface area. The sequence of HF-NaOH treatments alters the catalytic properties [20]. Pyrolysis of lignite blended with $CaSO_4$-rich ash had little effect at low temperatures (500 °C) on gas yield. However, the gas phase yield evidently increased at temperatures above 750 °C [21]. Coal bottom and fly ash were used as catalysts in the pyrolysis process. Better catalytic activity was found for bottom ashes than for fly ashes because they were rich in alkali and alkaline earth metal oxides [22]. Coal fly ash acts as a promoter of ketonization and esterification reactions, which was confirmed in corn stalk pyrolysis studies [23]. Wu et al. [24] investigated the effect of ZSM-5 and coal gasification ash on the pyrolysis process of cow manure. Increasing the catalyst–biomass ratio promoted the production of monocyclic aromatic hydrocarbons and polycyclic aromatic hydrocarbons. Among monoaromatic compounds, toluene represented more than a third of the compounds identified when the HZSM-5–rice husk ash catalyst was used [25]. The use of cobalt impregnated sludge ash catalyst was an effective method to improve the efficiency of syngas (H_2 + CO) from co-pyrolysis of municipal solid waste and biomass [26]. The catalyst containing 10 % cobalt was more effective in producing the synthesis gas than the catalyst containing 5 % cobalt. Therefore, it was concluded that cobalt promotes hydrogen production through the Diels-Alder-type aromatization reaction, dry reforming of methane, and dehydrogenation reactions. As Al-Rahbi and Wiliams [27] showed, nickel-impregnated ashes from waste derived fuel and end-of-life tyres were more effective in producing hydrogen from biomass than coal ash. It was beneficial for syngas production if the nickel loaded with ash did not exceed 20 % by weight [28]. Excess nickel loading reduced its dispersion in the ash and blocked the active sites. The catalytic performance decreased slightly during long-term use of ash as a catalyst. Recent studies also indicate that hydrogen production was promoted by an increase in the temperature of the catalytic reaction when tyre ash was the catalyst [29]. An interesting way to increase carbon monoxide production during the pyrolysis of fly ash-modified biomass was to change the reaction atmosphere from nitrogen to carbon dioxide [30]. CO efficiency was also positively correlated with the enrichment of biomass with ash mainly containing sodium and potassium. The mass of ash doped into the biomass to induce catalytic pyrolysis reactions should be carefully selected on the basis of the potassium/carbon mole ratio in the biomass [31]. Song et al. also reported that the pyrolysis gas was enriched in methane when fly ash was used as a catalyst [32]. Ash addition was less effective in promoting biochar yield and carbon conversion efficiency when ash-rich feedstocks were used. Catalytic pyrolysis of biomass over ZSM-5 doped with biomass ash increased the production of the aqueous phase and non-condensable gases compared to ZSM-5 not doped with ash. Unfortunately, the ash particles clearly poisoned the catalyst in subsequent cycles. As a result, the ZSM-5 ash-free catalyst was recommended for long-term reuse [33]. A summary of previous investigations into the pyrolysis of solid feedstocks over ash catalysts is shown in Table 1. As can be seen in Table 1, there was a lack of investigation for the long-term reuse of ash catalysts.

The identification of the research gap was an incentive for conducting research on the pyrolysis of waste biomass using ash as a catalyst. Additionally, for comparison, biomass pyrolysis was performed over a commercial catalyst. The results of this work pave the way for the development of sustainable solutions for the reuse of ashes as catalytic carriers for biomass pyrolysis.

2. Materials and methods

2.1. Biomass

Waste grass is a highly relevant and significant feedstock for pyrolysis to produce high-calorific fuels and valuable chemicals. Its rapid growth and cost-effectiveness compared to cereal straw or wood make it an attractive feedstock for sustainable energy production. Through pyrolysis, the waste grass can be converted to bio-oil, pyrolysis gas, and biochar, contributing to the reduction of waste and providing a renewable energy source. This process not only helps to manage agricultural waste, but also reduces the dependence on fossil fuels, aligning with global efforts toward green energy and reducing the carbon footprint. The raw material for the research was grass waste from a village near Krakow in Poland. The dried grass was ground and then sieved to obtain a repeatable fraction size from 250 to 500 μm. A photo of the grass sample is shown in Fig. 1. The proximate, ultimate, and component analyses of the grass are presented in Table 2. The grass was characterised by a low ash content (6 wt%). The carbon content in the sample was approximately 47 wt% and 6 wt% hydrogen.

Unfavourable elements such as sulphur and chlorine are also observed in grass. The grass belongs to lignocellulosic biomass, rich in cellulose 38 % and hemicellulose (27 %).

2.2. Reference composition of ash and catalysts

Currently, most car tyres are either incinerated or landfilled. In Poland, cement plants such as Górażdże and Dyckerhoff have installations that allow the co-incineration of whole car tyres. The resulting ash, which is rich in silicon and zinc, shows potential as a catalyst carrier. For this investigation, the shredded car tyres were incinerated in a muffle furnace at 815 °C in an air atmosphere, following the ISO 1171:2010 standard to determine ash in solid mineral fuels. The second material used in the experiment was a commercial catalyst. The purchased zeolite mordenite-sodium was manufactured by Thermo Scientific Chemicals (CAS: 1318-02-1). The zeolite mordenite-sodium is known for its large surface area, pore structure, and strong acidity, which makes it an effective catalyst for biomass pyrolysis. Fresh ash (ash_0) and zeolite (zeolite_0) prior to pyrolysis were calcined at 600 °C in a muffle furnace. A heating rate of 10 °C/min was used and after reaching the required temperature, the samples were kept for 4 h. After cooling, the samples were stored in a desiccator. As shown in Table 3, the main component of ash and zeolite is SiO_2. The high SiO_2 content is beneficial as it provides a stable matrix for the catalyst, enhancing thermal stability and resistance to sintering during pyrolysis. The zeolite contained 11.61 % Al_2O_3 while the ash contained only 1.36 %. Alumina enhances the acidity of the catalyst, which is crucial for breaking down large hydrocarbon molecules during pyrolysis. The calculated acidity of the catalysts expressed as the silica-to-alumina ratio: for ash, it was 112 and for zeolite it was 12. Reduced acidity could favour dehydrogena-

Table 1
The application of ash as a catalyst for solid raw material pyrolysis in previous research, where: AR, Auger reactor, BB, biomass bottom ash, BF, biomass fly ash leachate, CA, coal ash (unspecified type), Cats, catalyst, CB, coal bottom ash, CF, coal fly ash, CG, coal gasification ash, HDPE, high-density polyethylene, HFB, horizontal fixed-bed reactor, LDPE, low-density polyethylene, Nd, not determined, PA, paper sludge ash, RA, refuse-derived fuel ash, RM, raw material, SF, sludge fly ash, T_{cats}, catalyst temperature, T_p, pyrolysis temperature, TA, tyre ash, TSF, two-stage fixed-bed, TF, tube furnace and VFB, vertical fixed-bed.

RM	Cats	RM:Cats ratio	RM-Cats mixed	RM-Cats not mixed	Reactor type	T_p, (°C)	T_{cats}, (°C)	Reuse of Cats	Ref.
Coal	CF	3:1, 2:1, 1:1, 1:2, 1:3	✓	–	VFB	700–900	700–900	–	[20]
Coal	CA	1:3	✓	–	VFB	500–850	500–850	–	[21]
LDPE	CA, CB	1:0.15	✓	–	TF	550	550	–	[22]
Corn stalk	CF	2:1, 3:2 1:1, 1:2	✓	–	HFB	460–520	460–520	–	[23]
Cow manure	CG	2:1, 1:1, 1:2	–	✓	VFB	700	700	–	[24]
Micro-algae	RH	5:1	–	✓	TF	500	500	–	[25]
MSW/Pine sawdust	SF	3:1	–	✓	TSF	700	800	–	[26]
Wood	CA, TA, RA	1:1	–	✓	TSF	600	800	–	[27]
Rice Straw	CF	2:1	–	✓	HFB	550–800	550–800	✓	[28]
HDPE	TA, RA	0.2:1, 0.5:1, 1:1	–	✓	TSF	600	800-1000	–	[29]
Cedar bark	BF	Nd	✓	–	HFB	800	800	–	[30]
Softwood	BB	50:1, 20:1, 11:1, 3:1, 2:1	✓	–	AR	400-500	400-500	–	[31]
Wood chips	CF	10:1, 10:2, 10:3, 10:4, 10:5, 10:6, 1:1	✓	–	HFB	600	600	–	[32]
Herb residue	PA	1:1	–	✓	VFB	600	600-800	–	[34]
Grass	TA	1:1	–	✓	VFB	500	500	✓	this study

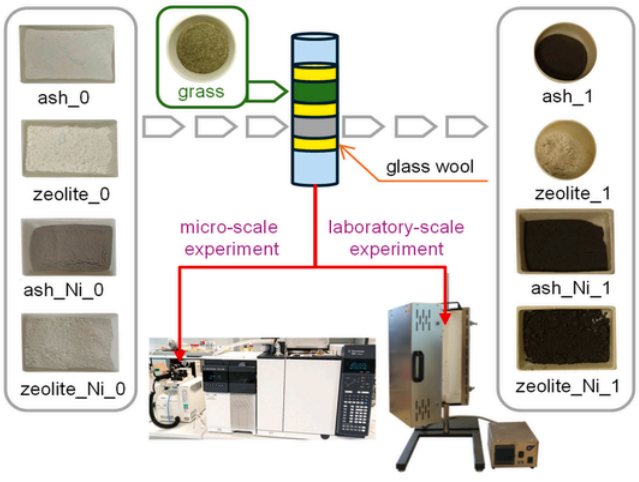

Fig. 1. Photographs of samples prepared for pyrolysis and experimental equipment for investigation on a micro– and laboratory–scale.

tion reactions over cracking, which could be desirable in processes aimed at producing olefins or other specific hydrocarbons. The zeolite contained 7.82 % Na_2O. In high-temperature processes, such as catalytic pyrolysis, the presence of sodium (Na^+) helps stabilise the zeolite framework by balancing negative charges on the aluminosilicate lattice. In mordenite, sodium ions replace some of the protons (H^+) typically present in the zeolite structure. The presence of metal oxides such as ZnO and Fe_2O_3 in tyre ash can improve the durability and activity of the catalyst by introducing additional active sites and enhancing the redox properties.

2.3. Catalyst preparation

The catalysts for the pyrolysis process were four samples: car tyre ash, zeolite mordenite-sodium, NiO supported on ash and NiO supported on zeolite mordenite-sodium-supported. The addition of nickel into the ash and zeolite support was achieved by an impregnation method [35]. Impregnation was carried out by dissolving 5.51 g of $Ni(NO_3)_2 \cdot 6H_2O$ in 100 ml of distilled water and adding 10 g of ash. The prepared mass proportions were used to obtain a 10 % nickel content in the catalyst. The aqueous solution was stirred magnetically at a speed of 300 rpm for 6 h, then heated to 70 °C, and kept at this temperature until the water evaporated. In the next stage, the sample was dried at 105 °C for 12 h and calcined at 600 °C for 4 h. As a result of calcination, nickel was bound to oxygen as NiO. Before being sent to pyrolysis, the ash-supported nickel catalyst was crushed in a mortar to obtain a fraction below 250 μm. The Ni impregnation of zeolite was carried out according to a similar procedure. Fresh catalysts, i.e. after calcination and before pyrolysis, were assigned the sample names ash_0, ash_Ni_0, zeolite_0, and zeolite_Ni_0. Catalysts after the first pyrolysis experiment (first cycle) were designated ash_1, ash_Ni_1, zeolite_1, and zeolite_Ni_1. The catalysts were then calcined according to the procedure described in this section, and used again for pyrolysis. The catalyst samples used for a second time for pyrolysis (second cycle) were named ash_2, ash_Ni_2, zeolite_2, and zeolite_Ni_2, respectively. Photographs of the prepared catalysts after calcination are shown in Fig. 1.

Table 2
Proximate, ultimate and component analyses of grass.

Proximate analysis, (air-dried basis, %)					
Moisture	Volatile Matter		Ash	Fixed carbon[a]	
9.28 ± 0.29	80.13 ± 0.04		6.19 ± 0.24	4.40 ± 0.58	
Ultimate analysis (dry base, %)					
Carbon	Hydrogen	Nitrogen	Sulphur	Chlorine	Oxygen[b]
46.54 ± 0.25	6.13 ± 0.04	2.26 ± 0.02	0.23 ± 0.01	0.27 ± 0.03	37.75 ± 0.18
Component analysis (air-dried basis, %)					
Cellulose	Hemicellulose		Lignin	Extractives[c]	
38.49 ± 0.68	27.12 ± 0.49		8.29 ± 0.38	10.63 ± 0.36	

Note: Values are presented as means ± standard deviation (n = 3). [a]Fixed carbon = 100 – Moisture – Volatile matter – Ash, [b]Oxygen – by difference, [c]Extractives = 100 – Cellulose – Hemicellulose – Lignin – M – A.

Table 3
Compositions of tyre ash and zeolite mordenite-sodium.

Component	ash_0	zeolite_0
	Content (wt.%)	
Na_2O	1.09	7.82
MgO	0.12	0.05
Al_2O_3	1.36	11.61
SiO_2	89.59	79.82
P_2O_5	0.04	0.01
SO_3	0.90	0.03
Cl	0.05	0.04
K_2O	0.13	0.05
CaO	0.71	0.03
TiO_2	0.10	0.36
Fe_2O_3	1.05	0.11
CuO	0.08	–
ZnO	4.51	–
ZrO_2	0.10	0.05
Other	0.17	0.02

2.4. Instrumental methods

A Leco CHNS 628 model elemental analyser was used for the ultimate analysis of raw material, char and oils. A muffle furnace (LIFT 3.0 - Neotherm Poland) was used for the proximate analysis according to the following standards: ISO 18134–3:2023 (moisture), ISO 18122:2022 (ash), ISO 18123:2023 (volatile matter). The ash from the passenger car tyres was obtained by incinerating crushed material at 815 °C according to the ISO 1171: 2010 standard. The analysis of grass fibre was carried out according to the standards ISO 13906:2009 and ISO 16472:2007. The pyrolytic gas was analysed using a gas chromatography system (Agilent Technology 7890A). The compositions of ash and zeolite were analysed using the X-ray fluorescence (XRF) spectroscopy technique. Measurements were performed with a WD-XRF ZSX Primus II Rigaku spectrometer (Rh lamp). Fresh and spent catalysts were analysed using X-ray diffraction with a Philips (Panalytical) X'Pert Pro X-ray diffractometer. Thermogravimetric (TG) analysis was performed using a Mettler Toledo STA apparatus for the study of grass pyrolysis. The investigations were carried out twice to ensure repeatability and good consistency with standard errors for temperature readings of ±1 °C. A Fourier-transform infrared (FT-IR) spectrometer (Bruker Alpha II) was used for the identification of functional groups and bond types present in biomass, chars, and oils. The determination of the concentration of Lewis and Brønsted acid centres on the surface of the catalysts was analysed using the FT-IR spectroscopic method of pyridine sorption on samples degassed under high vacuum conditions, at a temperature of 450 °C for 2 h. A Bruker FT-IR spectrometer, model Invenio, with an MCT detector was used.

2.5. Pyrolysis–gas chromatography/mass spectrometry analysis

The potential effect of the presence of different catalyst systems on the performance of grass pyrolysis was investigated on the basis of the coupled technique pyrolysis - gas chromatography - mass spectrometry (Py-GC/MS). A photograph of the equipment used is shown in Fig. 1. The tests were carried out using a pyrolizer unit (CDS Analytical, model 5200) coupled to a gas chromatograph unit (Agilent Technologies, model 7890B) and a mass spectrometer (Agilent Technologies, model 5977A). This work mainly aimed to assess the effect of the presence of various catalysts on the change in reaction pathways that occur during the pyrolysis of grass samples. The grass sample was approximately 500 μg. For all catalytic studies, the catalyst/grass mass ratio was equal ca. 1:1. The analyses were conducted under an inert atmosphere (He, grade: 6.0). The pyrolysis studies were carried out at 500 °C, which was selected based on the results of the TGA analysis when the major decomposition of the raw material was complete. The heating rate was equal to 100 °C/s with a hold time at the designed temperature of 30 s. The evolved products were transferred to the GC-MS analysis through a heated line kept at 325 °C. The GC was equipped with an Agilent HP-5MS capillary column with dimensions of 60 m × 0.25 mm × 0.25 μm. The GC oven temperature programme was as follows: (i) 40 °C with a holding time of 7 min; (ii) heating ramp from 40 °C to 300 °C at a rate of 4 °C·min^{-1}; (iii) isothermal held at 300 °C for 10 min. The MS spectra were interpreted based on the reference MS library (chemical base NIST14). Details of the procedure can be found in previous reports. The identified peaks were grouped into the following types of compounds: (i) gaseous products, (ii) oxygen compounds (aldehydes, alcohols, ketones, acids, esters), and hydrocarbons (aliphatic, cyclic, and aromatic). The share of each compound was calculated as a ratio of the peak area of all compounds within the group to the total peak area of all compounds in all groups.

2.6. Pyrolysis in a vertical fixed-bed reactor

The grass pyrolysis experiments were carried out in a vertical fixed-bed furnace from the Czylok model RSD 50x414/120 (see the photo shown in Fig. 1). Nitrogen was the carrier gas for the pyrolysis process, with a flow rate of 150 ml/min. For each measurement series, 3 g of biomass sample and 3 g of catalyst sample were used, which corresponded to a biomass/catalyst ratio of 1:1. Samples were placed in two distinct layers, separated by high-temperature glass wool. Before heating the reactor, the samples were purged with nitrogen for 15 min to remove any residual air. The grass and catalyst were heated at a rate of 30 °C/min to a temperature of 500 °C, and then kept for 10 min in a constant temperature zone of the reactor. The bio-oil condensed in an ice-filled cooler was weighed to calculate the pyrolysis yield. The un-

condensed gases were collected in a Tedlar bag for chromatographic analysis. After the reactor was cooled in an N_2 atmosphere, the char was weighed.

3. Results and discussion

3.1. Thermogravimetric analysis of grass

Preliminary studies of grass pyrolysis included thermogravimetric analysis. Fig. 2 shows the TG (thermogravimetric) and DTG (derived thermogravimetry) curves of the pyrolysis process for a heating rate of 10 °C/min with a nitrogen flow of 40 ml/min. At 500 °C the solid residue was 29 %. In the DTG curve, a clear peak was observed at 319 °C, representing the decomposition of cellulose and hemicellulose, the main components of grass [36]. The continued weight loss up to 500 °C was likely due to lignin breakdown, which decomposes over a wider temperature range. The last stage of grass pyrolysis above 500 °C represented thermal annealing of char.

3.2. Fourier transform infrared spectroscopy of grass and char

Fourier Transform Infrared (FT–IR) spectra were used to demonstrate the chemical transformations that occur during the pyrolysis of grass, leading to the formation of char. Fig. 3 shows the FT–IR spectra, which provide information about the functional groups present in grass and char. Six absorbance peaks were identified in the grass sample, respectively for wavenumbers: i) 3355 cm^{-1} – broad peak due to O–H stretching, indicative of hydroxyl groups, which are abundant in cellulose and hemicellulose in the grass, ii) 2919 and 2851 cm^{-1} – peaks corresponding to C–H stretching in aliphatic groups $–CH_2–$ and $–CH_3$, iii) 1632 cm^{-1} – peak associated with the C = C stretching vibrations of aromatic rings or alkenes, potentially from lignin or unsaturated compounds, iv) 1028 cm^{-1} C–O–C stretching vibrations, commonly found in polysaccharides like cellulose, and v) 567 cm^{-1} C–Cl stretching, although chlorinated compounds are less common in natural biomass, it could indicate trace contamination. The spectral line representing the char in the wavenumber range of 3600 to 2800 cm^{-1} has become flattened compared to the grass. The flattening indicates the loss of hydroxyl groups as a result of dehydration and reduction of aliphatic groups. In the double bond region, a peak was observed at 1576 cm^{-1}. The peak has shifted from 1632 cm^{-1}, which could be due to changes in chemical structure, such as the formation of more condensed aromatic structures [37]. The fingerprint region revealed the highest number of peaks. They were as follows: O–H bending vibrations (1392 cm^{-1}), C–O stretching (1254 and 1062 cm^{-1}), out-of-plane C–H bending vibrations (873 and 834 cm^{-1}), C = C bending (693 cm^{-1}), and C–Cl (567 cm^{-1}). Decrease in C–O–C and C–O stretching vibrations, indicating the breakdown of cellulose and hemicellulose [38]. The result of pyrolysis was an overall reduction in peak intensities, reflecting the transformation of complex organic compounds into simpler structures, primarily carbonaceous char.

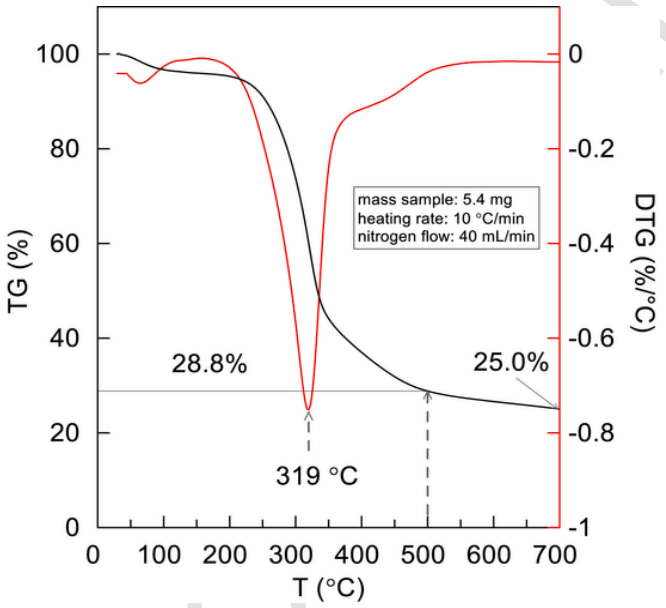

Fig. 2. TG and DTG curves of the grass pyrolysis process at 10 °C/min.

3.3. Catalyst characterization

Fresh and spent catalysts were analysed using Py-FT-IR to determine acid sites. Fig. 4a–b) shows the Py-FT-IR spectra of the catalysts in the range of 1700–1400 cm^{-1} to illustrate the differences in the intensities of the C = C vibration bands of the pyridine (Py) ring. The spectra were spread out, and baseline correction was performed for the entire spectral range for a better comparison of the spectra. The concentration of Brønsted and Lewis acid sites was determined in quantitative IR studies of pyridine [39]. Table 4 contains the concentration values calculated on the basis of the intensity of the Py bands associated with the Brønsted centres (1544 cm^{-1}, PyH^+) and with the Lewis centres (1446 cm^{-1}, PyL). As can be seen from Fig. 4a–b) and Table 4, Brønsted acid sites were present only in the zeolite_Ni_0 and zeolite_Ni_2 samples. As a result of the nickel support on the ash, the concentration of Lewis acid sites increased twofold.

The concentration of PyL in zeolite increased significantly after the introduction of nickel, increasing from 25 μmol/g to 107 μmol/g. Interestingly, the concentration of Lewis acidic sites in the ash_2, zeolite_2 and zeolite_Ni_2 pyrolysis catalysts was increased. The possibility of increasing Lewis acid sites should be thoroughly investigated in the future. The formation of additional Lewis acid sites is possible by exposing the catalyst to water vapour [40] or by introducing metal ions to the surface [41].

The X-ray diffraction analysis for calcined fresh and spent catalysts is shown in Fig. 5. In ash_0, the SiO_2 peak at 21.9° is the most intense.

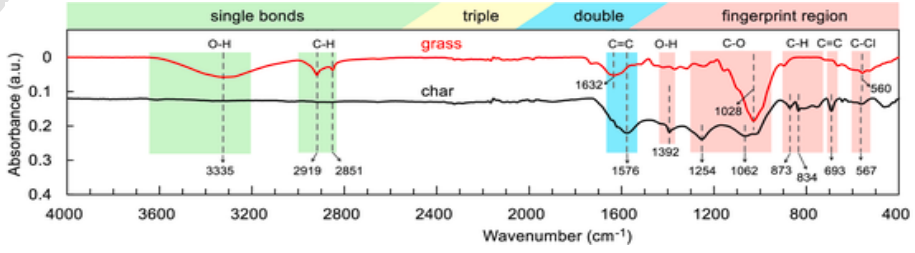

Fig. 3. Fourier transform infrared spectra of grass and char.

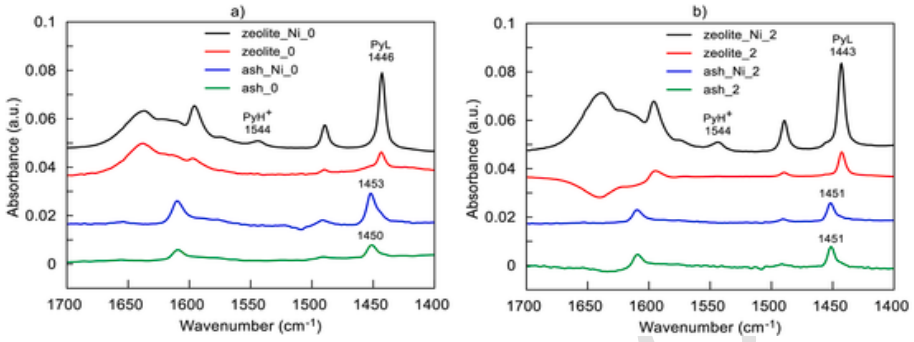

Fig. 4. Py-IR spectra of catalyst a) fresh, b) spent, after the second cycle.

Table 4
Total acidity of the fresh and spent catalyst.

Catalyst	B-acid (μmol/g)	L-acid (μmol/g)
ash_0	0	20
ash_Ni_0	0	40
zeolite_0	0	25
zeolite_Ni_0	9	107
ash_2	0	25
ash_Ni_2	0	35
zeolite_2	0	45
zeolite_Ni_2	11	150

After the second cycle (ash_2), the peak is much lower, which may be due to the catalyst being clogged with coke. The diffraction peaks shown around 25.6°, 31.6, °34.0° and 39° were related to the presence of $Zn_2(SiO_4)$, which is in agreement with the XRF results in which zinc was identified. After the ash was impregnated with nickel, diffraction peaks of NiO were identified in the ash_Ni and ash_Ni_2 samples. The peaks were weak and broad, indicating that the active Ni sites were well dispersed on the support [35].

In turn, the XRD diffraction patterns of the zeolites revealed numerous peaks originating from mordenite $(Ca,Na)Al_2Si_{10}O_{24} \cdot 7H_2O$. Compared to fresh zeolites (zeolite_0 and zelite_Ni_20), the XRD patterns of spent zeolites showed the same diffraction peaks with reduced intensity.

3.4. Pyrolysis–gas chromatography–mass spectrometry

Fig. 6a–c) shows the results of Py-GC-MS analysis, indicating the area share (%) of different groups of compounds released during non-catalytic pyrolysis of grass, and catalytic pyrolysis over ash_1, ash_Ni_1, zeolite_1, and zeolite_Ni_1. The results are divided into three groups: general compounds (Fig. 6a), specific oxygen-containing compounds (O-compounds) (Fig. 6b), and types of hydrocarbons (Fig. 6c). The predominant group of compounds is shown in Fig. 6a). For individual groups, Table 5 lists the main component and relative share. In gaseous compounds, the main compound was carbon dioxide. The relative share of carbon dioxide increased by nearly 27 % during pyrolysis over zeolite_Ni_1 compared to non-catalityc pyrolysis. Grass decomposition occurs primarily via the decarboxylation route, which explains the dominant share of carbon dioxide among gaseous products. The production of these gaseous compounds was more pronounced with the ash- and zeolite-supported nickel catalyst, indicating significant cracking of hydrocarbon [34]. A detailed analysis of the gas composition is provided in Section 3.5.3. The second major group of compounds were O-compounds. Catalytic pyrolysis effectively reduces the share of oxygenates with nickel supported on ash and zeolite catalysts, showing even more pronounced effects. This reduction is likely due to the presence of nickel, which partially converts oxygenates to ethers [13].

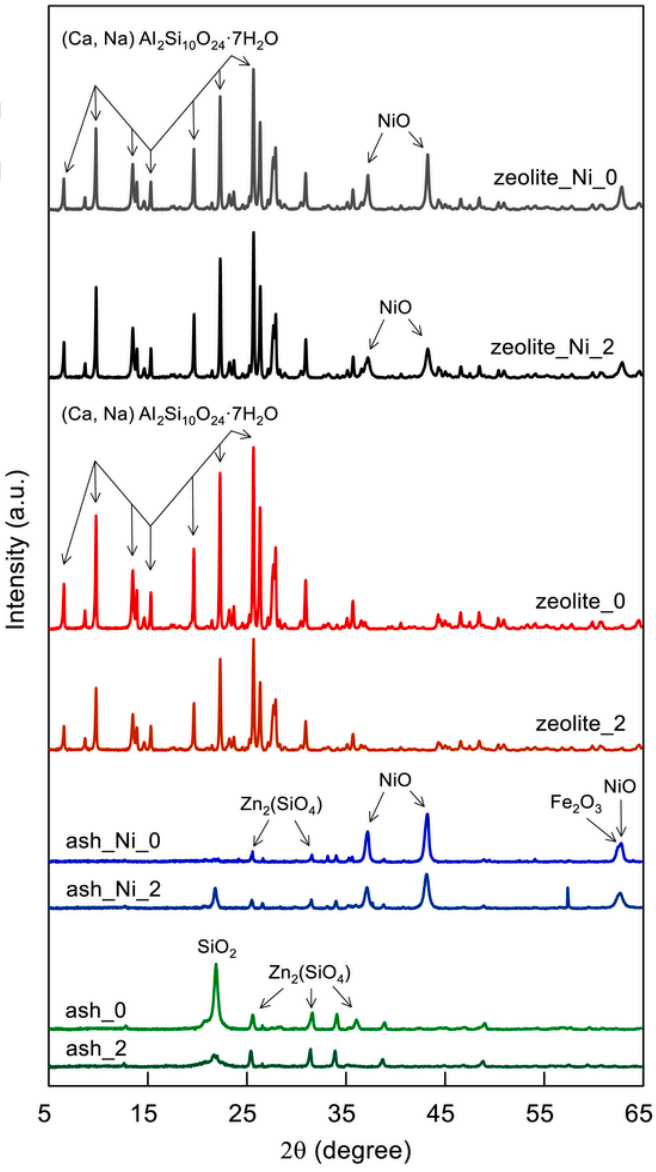

Fig. 5. XRD pattern of fresh catalysts (ash_0, ash_Ni_0, zeolite_0, zeolite_Ni_0) and spent catalysts (ash_2, ash_Ni_2, zeolite_2, zeolite_Ni_2).

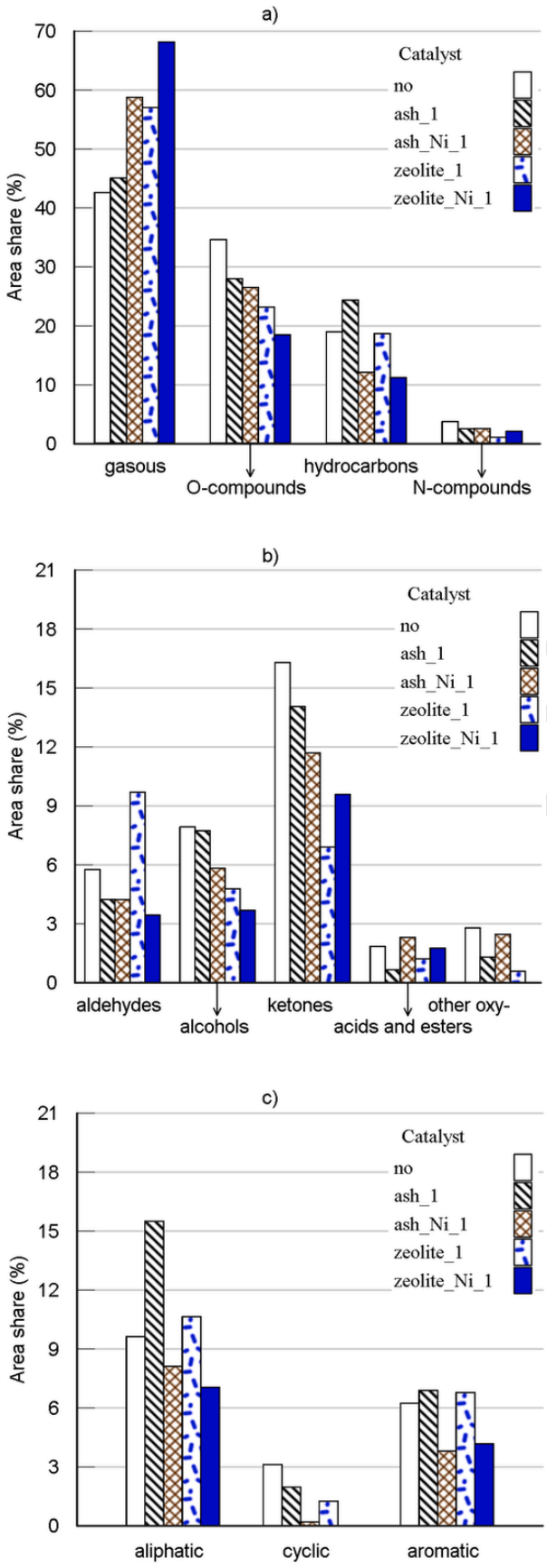

Fig. 6. The influence of the catalyst used on the composition of grass pyrolysis products: a) all product groups, b) O-compounds, c) hydrocarbons.

Table 5
Main components identified in individual groups of compounds and their relative share.

Catalyst type		no	ash_1	ash_Ni_1	zeolite_1	zeolite_Ni_1
Product groups	Main component	Relative share (%)				
Gaseous	carbon dioxide	29.48	41.71	51.65	52.89	56.39
O-compounds						
Aldehydes	acetaldehyde	3.56	2.91	3.29	7.74	2.35
Alcohols	1-octanol	1.67	1.42	1.28	0.90	0.92
Ketones	1-hydroxy-2-propanone	8.54	6.78	7.08	3.39	5.92
acids and esters	acetic acid	0.69	0.21	1.91	0.43	1.57
other oxy-	3-methylfuran	0.21	0.78	1.15	0.46	0
Hydrocarbons						
Aliphatic	butane	5.84	7.92	6.48	6.57	5.72
Cyclic	–	–	–	–	–	–
Aromatic	toluene	3.50	3.86	1.94	4.09	2.55
N-compounds	1,4-dimethyl-pyrazole,	2.22	1.85	1.61	1.09	1.58

These ethers then undergo carbonyl alkylation reactions with the carbonyl groups in the biomass. NiO supported on zeolite catalysts (compared to MgO, CaO, and Co_3O_4) was characterized by the highest conversion of oxygenates [42]. For non-catalytic pyrolysis, hydrocarbons accounted for 19 % of the products. Ash was the most effective catalyst for promoting the formation of hydrocarbons. However, when pyrolysis was conducted over nickel supported on catalyst, the hydrocarbons share was significantly reduced to approximately 12 %, which is lower than that of non-catalytic pyrolysis. Nitrogen compounds formed a minor fraction, confirming the low protein content of the grass.

The formation of O-compounds such as aldehydes, ketones, alcohols, carboxylic acids, and esters is depicted in Fig. 6b. Those are typical products of saccharide decomposition pathways, the main building blocks (hemicellulose, cellulose) of biomass [43]. Key observations related to catalyst include suppression of alcohols, ketones, and other oxy-compounds, consistent with the literature [33]. The ketone with the highest relative share was 1-hydroxy-2-propanone. As Usino et al. [44] stated, 1-hydroxy-2-propanone was one of the main products obtained from pyrolysis of a xylan-lignin blend. The most abundant acid compound in terms of relative share was acetic acid. Simultaneously, nickel supported catalysts promoted the formation of acids, which has been previously confirmed [45]. Among the hydrocarbons released (Fig. 6c), the aromatic and aliphatic structures were the most prevalent and stable. Notably, the presence of nickel oxide on both supports led to a noticeable decrease in both the aromatic and aliphatic groups. Butane and toluene were the predominant compounds in the aliphatic and aromatic groups, respectively. No dominant compound was identified among the cyclic aromatic groups (3-(2-propenyl)cyclopentene for non-catalytic pyrolysis and bi-2-cyclohexen-1-yl for pyrolysis over ash and zeolite).

3.5. Pyrolysis in a fixed-bed reactor

3.5.1. Yield of products

The char and condensing bio-oil were weighed after each measurement series. The masses of char and bio-oil related to the mass of the grass sample allowed us to calculate their yields. However, the yield of pyrolysis gas was determined as a difference of up to 100 %. The yields of the pyrolysis products after the first cycle are shown in Fig. 7a) and after the second cycle in Fig. 7b). As shown in Fig. 7a), almost 49 % was the gas yield from non-catalytic pyrolysis. The use of ash as a catalyst

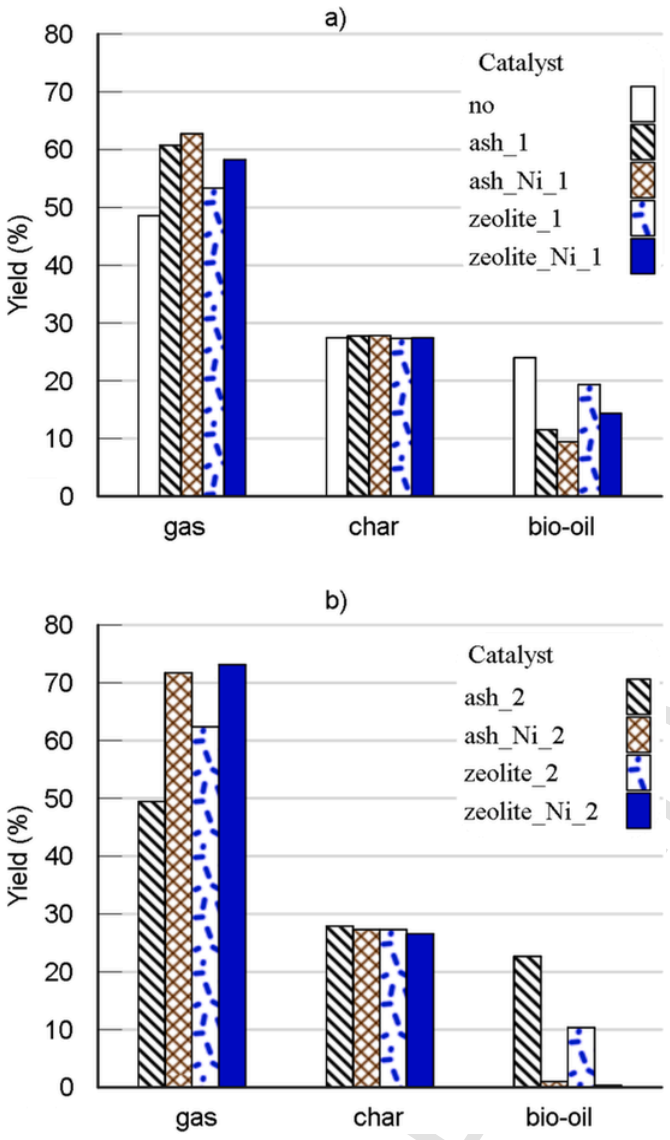

Fig. 7. Yields of pyrolysis products after a) first cycle, b) second cycle.

for the first pyrolysis cycle increased the gas yield to 61 % and was more effective in gas production than zeolite. Ash and nickel supported on zeolite promoted higher gas yields. These conclusions are consistent with the findings of Al-Rahbi and.

Williams [27], who indicate that nickel supported on ash catalysts results in a higher gas yield compared to non-nickel-impregnated ash and non-catalyst pyrolysis. For catalytic and non-catalytic pyrolysis, the char yield was similar (~27 %), which means that the trends of increase/decrease in the bio-oil yield were contrary to the pyrolysis gas yields. The second cycle with the ash_2 catalyst (Fig. 7b) showed a 11 % decrease in gas yield. On the contrary, the remaining catalysts exhibited increased yields: 9 % for zeolite_2 and ash_Ni_2, and 15 % for zeolite_Ni_2. In the second cycle, the ash_Ni_2 and zeolite_Ni_2 catalysts showed almost complete cracking of the bio-oil (yield was below 1 %). Bio-oil includes an aqueous and organic phase. Their yields are closely related to the pyrolysis conditions and the catalyst used. On the one hand, after subsequent catalyst regenerations, Yildiz et al. [46] reported a decrease in the yield of the organic phase and an increase in the yield of the aqueous phase. However, there are also reports in which opposite directions of changes in organic and water phase yields were obtained, for example [47].

3.5.2. Ultimate analysis of char and spent catalysts

Fig. 8 illustrates the ultimate analyses of chars (carbon, hydrogen, and nitrogen contents) from grass pyrolysis and grass pyrolysis over catalysts: ash_1, ash_Ni_1, zeolite_1, and zeolite_Ni_1. The ultimate analysis was performed in triplicate, and the bars represent the standard deviation of the mean. The analysis of chars was carried out for the first and second cycles. However, the composition of the chars did not change after reusing the catalysts. Char from noncatalytic pyrolysis of grass contained approximately 66.8 % carbon. The carbon content in the char increased with the use of all types of catalysts analysed. Specifically, by pyrolysis of grass over ash_1 and the ash_Ni_1 catalyst, the carbon content increased to approximately 68 %, indicating that nickel supported on ash did not significantly affect the carbon content. The highest carbon content (68.6 %) was observed during grass pyrolysis over zeolite, while nickel supported on zeolite slightly reduced the carbon content. This indicated that zeolite was more effective in carbonisation of the char. The increase in carbon content in chars during catalytic pyrolysis can be attributed to two main factors: i) changes related to the flow of hot pyrolysis gases, and ii) catalytic reactions on the surface of the char. The use of a catalyst in the pyrolysis reactor, placed beneath the grass sample, formed resistance to the flow of pyrolysis gases. This results in plug flow and pressure change within the high-temperature ceramic wool-filled space between the catalyst and the grass sample. Additionally, the C/H molar ratio exceeding 1.7 indicated the presence of aromatic compounds in all char samples [48].

Yildiz et al. [33] found that the presence of ash can improve the carbon content of char by promoting secondary reactions that favour carbon formation. Ash used as a catalyst facilitates the breakdown of larger organic molecules into smaller ones. Sodium-mordenite zeolite promotes the cracking, polymerisation, and aromatization reactions, which contribute to the formation of more condensed and stable carbon structures [49]. Zeolite, in particular, has been noted for its ability to produce chars with a higher carbon content due to its strong acidic sites, which are effective in catalysing the breakdown of organic matter into carbon-rich compounds [50]. The presence of sodium in zeolites also affects catalytic activity, which could improve carbon formation by modifying acidity and catalytic pathways [51]. However, the influence of catalysts on the hydrogen and nitrogen content in the chars was different. For hydrogen and nitrogen, the differences among the investigated catalytic conditions are less pronounced. The hydrogen content remains relatively stable, approximately 3 % across all samples. Similarly, the nitrogen content was consistent, slightly above 2 %, with minimal vari-

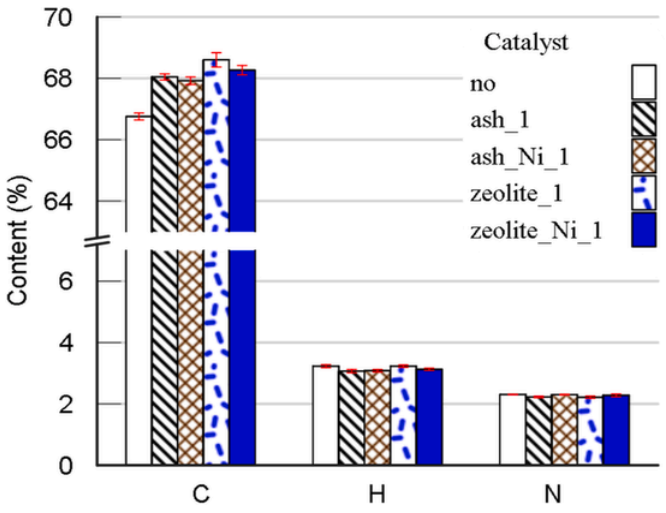

Fig. 8. Ultimate analysis of chars.

ation between different catalytic conditions. This stability in hydrogen and nitrogen content might be due to the inherent properties of the grass feedstock and the specific conditions of pyrolysis, which do not favour significant changes in these elements despite the presence of different catalysts.

The presence of carbon in the catalysts reflects the formation of coke. To determine the coking of the catalysts after the first cycle and reuse, an ultimate analysis was performed. Before reuse of the catalysts for pyrolysis, they were calcined at 600 °C for 4 h in an air atmosphere. The ultimate analysis of the spent catalysts after the first cycle is shown in Fig. 9a) and after the second cycle in Fig. 9b). As illustrated in Fig. 9a), the carbon content in the catalysts first used for pyrolysis varied depending on the type of catalyst. The ash_1 catalyst exhibited the highest carbon content at 3.0 %, which decreased slightly to 2.7 % for the ash_Ni_1 sample. The zeolite_1 contained 1.84 % carbon, while the zeolite_Ni_1 catalyst showed an increase in carbon content of 2.40 %. This indicates that nickel impregnation promotes coking in the zeolite and inhibits coking in the ash. The resistance to coke formation has increased due to the stabilising effect of nickel supported on the catalyst [52]. Regarding hydrogen content, both zeolite_1 and zeolite_Ni_1 catalysts displayed higher hydrogen content compared to those of the ash-based catalysts. However, there was a notable decrease in the hydrogen content after nickel impregnation. The nitrogen content in all samples was the lowest, ranging from 0.11 % to 0.23 %. These findings suggest that the addition of nickel significantly influences the elemental composition of the spent catalysts. This effect is likely due to alterations in the surface chemistry and catalytic properties induced by nickel. The observed changes in the elemental content indicate that both the type of catalyst and the presence of nickel play crucial roles in determining the catalytic behaviour and the resulting elemental composition, thereby impacting the efficiency and selectivity of the pyrolysis process. The content of carbon, hydrogen, and nitrogen after reusing catalysts for grass pyrolysis is shown in Fig. 9b). With the exception of zeolite_2, the spent catalysts had significantly lower carbon contents by approximately 0.5–0.7 % compared to their first use. This trend is different from expectations, but was observed in studies [48,53].

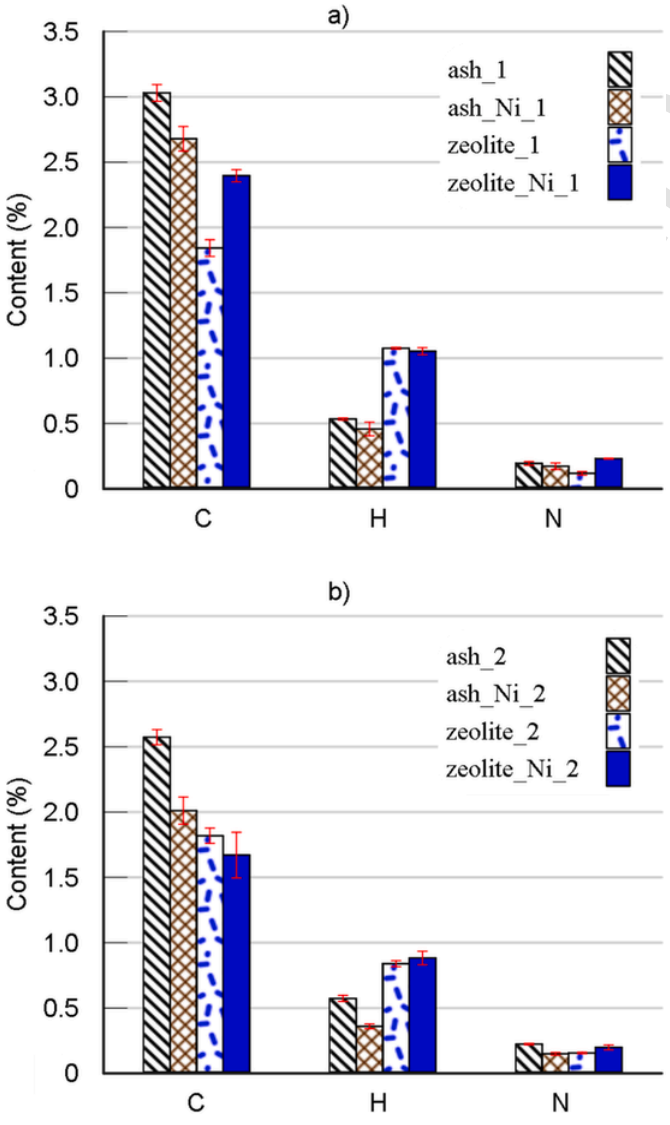

Fig. 9. Carbon, hydrogen and nitrogen content in spent catalysts after a) first cycle, b) second cycle.

The formation of coke is evidenced by the accumulation of carbon on the catalysts, with an increasing content observed as the zeolites are reused and progressively deactivated. Deactivation through coking involves the development of carbonaceous deposits, that gradually obstruct the surface and block the pores, resulting in a reduction in the number of accessible active sites and, consequently, a loss of catalytic activity. Moreover, less carbon was deposited on ash_Ni_2 and zeolite_Ni_2 compared to zeolite_2 and ash_2. At the same time, reduced hydrogen content was found for ash_Ni_2, zeolite_2 and zeolite_Ni_2. The molar H/C ratio was greater than 2 for ash catalysts, and >5 for zeolite catalysts. No significant changes were observed after the second cycle. The formed coke is classified as light aliphatic coke (H/C > 1) [54].

3.5.3. Pyrolysis gas composition

The distribution of gas products with different catalysts is presented in Fig. 10a–b). Gaseous compounds include CO_2, CO, H_2, CH_4, and higher hydrocarbons such as C_2H_6, C_2H_4, C_4H_{10} and C_3H_6. As a result of relatively low individual yields of higher hydrocarbons, these data are presented in summary form as C_xH_y. Following the first cycle of the process, the CO_2 yield increased from 37.5 % to 50.5 % during pyrolysis over zeolite, while it decreased to 4.1 % during pyrolysis over ash. The change in CO_2 content is accompanied by a corresponding change in other compounds, including CO (49.9 % for non-catalyst, 57.9 % for ash, 15 % for zeolite) and CH_4 (9.7 % for non-catalyst, 22.6 % over ash, 11.0 % over zeolite). The catalytic pyrolysis process yielded an increase in the hydrogen content. In the case of blank pyrolysis, without catalyst, the hydrogen yield was 2.1 %. In contrast, in the case of pyrolysis over ash_Ni_1 catalyst, the yield of hydrogen was 16.4 %. Furthermore, the methane content decreased compared to that of other catalysts. This phenomenon may be related to the reaction between methane and oxygen ($CH_4 + 0.5O_2 \rightarrow CO + 2H_2$) [55], as well as the influence of Ni on hydrogen production [56]. As evidenced by the aforementioned studies, the presence of nickel has been found to result in a decrease in liquid products concomitant with an increase in gas production, accompanied by a parallel increase in hydrogen yield [57]. The second cycle of experiments revealed a significant change in the concentration of CO_2 in the system. Pyrolysis over zeolite_Ni_2 resulted in a significant increase in the CO_2 content, from 21.6 % to 88 %. At the same time, there was a notable decrease in CO, CH_4 and H_2 concentrations, from 45.6 %, 19.3 %, and 10.5 %, respectively, to 0 %. These observations can be attributed to the reduced number of acid catalyst sites, which makes it difficult to react between CO_2 and the catalyst, preventing the formation of other compounds. Furthermore, the high yield of higher hydrocarbons, which cannot react with a clogged zeolite catalyst (zeolite_Ni_2 in the second cycle), provides additional evidence. The calculated higher heating values (HHV) of the pyrolysis gases were 11.3 MJ/m^3 without catalyst, 21.1 MJ/m^3 with ash_1, and 20.3 MJ/m^3 with ash_2. Furthermore, during the second cycle, a reduction in the HHV of

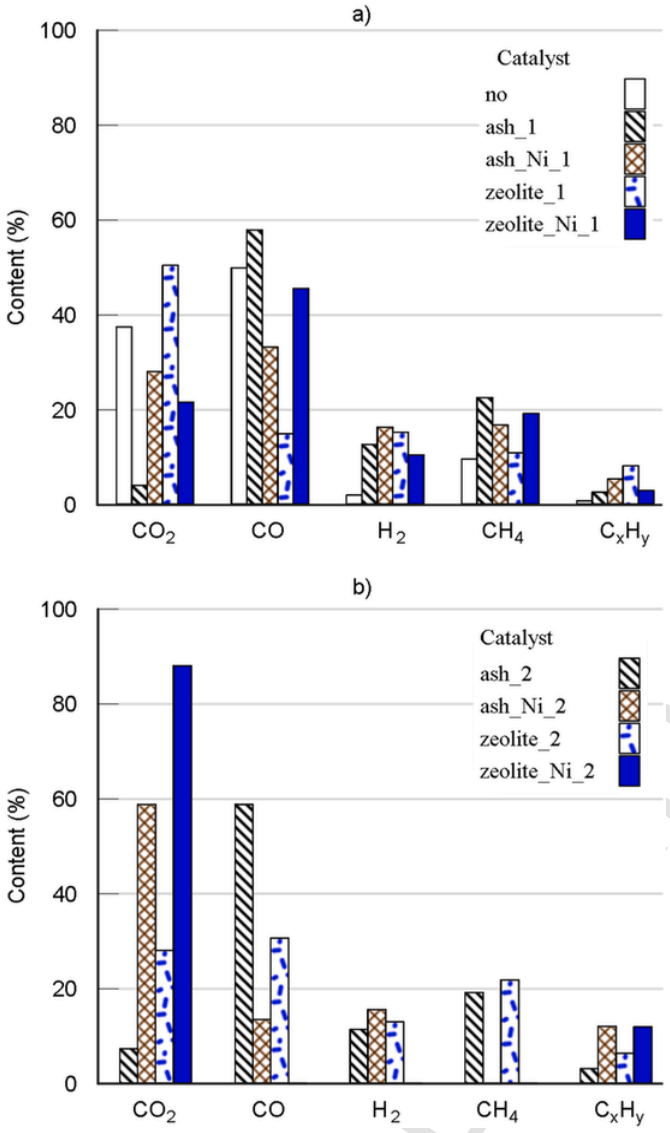

Fig. 10. Composition of the pyrolysis gas during: a) first cycle of catalysts, b) second cycle of catalysts.

the gas was observed for ash_Ni_2, (18.7 MJ/m^3) compared to the first cycle for ash_Ni (19.0 MJ/m^3).

4. Conclusions

This study examined the non-catalytic and catalytic pyrolysis of grass at 500 °C using four types of catalysts: car tyre ash, zeolite mordenite-sodium, NiO supported on tyre ash and NiO supported on zeolite mordenite-sodium. Additionally, spent catalysts were regenerated and reused for pyrolysis.

Tyre ash emerged as a promising candidate for use as a catalyst carrier. The addition of Ni to the catalysts notably increased the concentration of Lewis acid sites. Zeolite was found to be the most effective catalyst for promoting the formation of aldehydes, while ash was more effective for hydrocarbon production. The yields of the pyrolysis gas using nickel supported catalysts were significantly higher in the second cycle than in the first. Meanwhile, zeolite was more effective than ash in increasing char yield. The char produced over catalysts had a higher carbon content than that produced in the non-catalytic process. The carbon content in the catalysts after the second pyrolysis cycle was lower than after the first cycle, indicating resistance to coke formation. Analyses of the pyrolysis gas showed that the use of catalysts in the first cycle significantly promoted the formation of hydrogen. However, considering the reuse of catalysts and the content of flammable components (especially carbon monoxide), the long-term use of ash as a catalyst appears to be the most advantageous.

The use of tyre ash as a catalyst for grass pyrolysis offers significant cost, efficiency, and sustainability benefits. Economically, tyre ash is a readily available and inexpensive material, which reduces the overall cost of the pyrolysis process. Its ability to maintain catalytic properties for long-term use without degradation ensures consistent quality of the pyrolysis products, enhancing the efficiency and reliability. This stability minimises the need for frequent catalyst replacement, further lowering operational costs. From a sustainability perspective, the use of ash as a catalyst promotes a circular economy by repurposing waste materials, reducing landfill use, and mitigating the environmental impact. Furthermore, efficient conversion of grass into valuable fuels and chemicals through this method supports the transition to renewable energy sources, aligning with global sustainability goals and reducing dependence on fossil fuels.

CRediT authorship contribution statement

Wojciech Jerzak: Writing – original draft, Software, Resources, Methodology, Formal analysis, Conceptualization. **Małgorzata Sieradzka:** Methodology, Investigation, Formal analysis, Data curation. **Mariusz Wądrzyk:** Methodology, Investigation, Formal analysis, Data curation. **Aneta Magdziarz:** Writing – review & editing, Supervision, Project administration, Investigation.

Declaration of competing interest

The authors declare that they have no known competing financial interests or personal relationships that could have appeared to influence the work reported in this paper.

Acknowledgement

This research was funded by the National Science Centre of Poland [grant no. 2020/39/B/ST8/00883].

The authors also thank Prof. Marcin Gajek from AGH University of Krakow for carrying out the XRD studies of the catalysts and for his assistance in interpreting the results.

References

[1] European Environmental Agency, Share of energy consumption from renewable sources in Europe, https://www.eea.europa.eu, 2024.
[2] V. Avitabile, S. Mubareka, E. Baldoni, Biomass Supply and Uses in the EU - Summary for Policymakers, Joint Research Centre, European Commission, 2023, https://doi.org/10.2760/368529.
[3] P. Lisbona, S. Pascual, V. Pérez, Waste to energy: trends and perspectives, Chem. Eng. J. Adv. 14 (2023) 100494, https://doi.org/10.1016/j.ceja.2023.100494.
[4] S. Jha, S. Nanda, B. Acharya, A.K. Dalai, A review of thermochemical conversion of waste biomass to biofuels, Energies 15 (2022) 1–23, https://doi.org/10.3390/en15176352.
[5] M.K. Awasthi, T. Sar, S.C. Gowd, K. Rajendran, V. Kumar, S. Sarsaiya, Y. Li, R. Sindhu, P. Binod, Z. Zhang, A. Pandey, M.J. Taherzadeh, A comprehensive review on thermochemical, and biochemical conversion methods of lignocellulosic biomass into valuable end product, Fuel 342 (2023) 127790, https://doi.org/10.1016/j.fuel.2023.127790.
[6] C.A. García-Velásquez, C.A. Cardona, Comparison of the biochemical and thermochemical routes for bioenergy production: a techno-economic (TEA), energetic and environmental assessment, Energy 172 (2019) 232–242, https://doi.org/10.1016/j.energy.2019.01.073.
[7] N. Almagro-Herrera, S. Lozano-Calvo, A. Palma, J.C. García, M.J. Díaz, Assessing the influence of biomass origin and fractionation methods on pyrolysis of primary biomass fractions, Fuel 367 (2024) 131501, https://doi.org/10.1016/j.fuel.2024.131501.
[8] P.A. Østergaard, N. Duic, Y. Noorollahi, S. Kalogirou, Advances in renewable energy for sustainable development, Renew. Energy 219 (Part) (2023) 119377, https://doi.org/10.1016/j.renene.2023.119377.

[9] M.M. Hasan, M.G. Rasul, M.I. Jahirul, M. Mofijur, Fuelling the future: unleashing energy and exergy efficiency from municipal green waste pyrolysis, Fuel 357 (2024) 129815, https://doi.org/10.1016/j.fuel.2023.129815.

[10] W. Jerzak, M. Reinmöller, A. Magdziarz, Estimation of the heat required for intermediate pyrolysis of biomass, Clean Technol. Environ. Policy 24 (2022) 3061–3075, https://doi.org/10.1007/s10098-022-02391-1.

[11] Y. Wu, H. Wang, H. Li, X. Han, M. Zhang, Y. Sun, X. Fan, R. Tu, Y. Zeng, C.C. Xu, X. Xu, Applications of catalysts in thermochemical conversion of biomass (pyrolysis, hydrothermal liquefaction and gasification): a critical review, Renew. Energy 196 (2022) 462–481, https://doi.org/10.1016/j.renene.2022.07.031.

[12] A. Alagumalai, B. Devarajan, H. Song, Unlocking the potential of catalysts in thermochemical energy conversion processes, Catal. Sci. Technol. 13 (2023) 5632–5653, https://doi.org/10.1039/d3cy00848g.

[13] X. Yang, J. Zhang, J. Zheng, Z. Liu, J. Liu, S. Li, Y. Ye, W. Xie, J. Fan, H. Lan, D. Wang, Z. Zheng, In-situ and ex-situ catalytic pyrolysis of cellulose to produce furans over red mud-supported transition metal catalysts, J. Anal. Appl. Pyrolysis 169 (2023) 105830, https://doi.org/10.1016/j.jaap.2022.105830.

[14] L.G. Moura, G.E.S. dos Santos, H.O. Alves, J.Z. Marinho, M.A.S. Barrozo, A.O.T. Patrocinio, F.B. Noronha, C.E. Hori, Hydrogenation of guaiacol and pyrolysis of biomass using nickel and niobium-based catalysts, Catal. Lett. (2023), https://doi.org/10.1007/s10562-023-04500-1.

[15] W. Jerzak, N. Gao, I. Kalemba-Rec, A. Magdziarz, Catalytic intermediate pyrolysis of post-extraction rapeseed meal by reusing ZSM-5 and Zeolite Y catalysts, Catal. Today 404 (2022) 63–77, https://doi.org/10.1016/j.cattod.2021.10.023.

[16] D.K. Ratnasari, W. Yang, P.G. Jönsson, Two-stage ex-situ catalytic pyrolysis of lignocellulose for the production of gasoline-range chemicals, J. Anal. Appl. Pyrolysis 134 (2018) 454–464, https://doi.org/10.1016/j.jaap.2018.07.012.

[17] O. Norouzi, S. Taghavi, P. Arku, S. Jafarian, M. Signoretto, A. Dutta, What is the best catalyst for biomass pyrolysis? J. Anal. Appl. Pyrolysis 158 (2021) 105280, https://doi.org/10.1016/j.jaap.2021.105280.

[18] J. Lehmusto, F. Tesfaye, O. Karlström, L. Hupa, Ashes from challenging fuels in the circular economy, Waste Manag. 177 (2024) 211–231, https://doi.org/10.1016/j.wasman.2024.01.051.

[19] K. Gao, M.C. Iliuta, Trends and advances in the development of coal fly ash-based materials for application in hydrogen-rich gas production: a review, J. Energy Chem. 73 (2022) 485–512, https://doi.org/10.1016/j.jechem.2022.05.016.

[20] X. Chen, X. Zhang, J. Deng, Y. Feng, X. Fu, S. Yuan, Application study of pyrolysis and steam gasification of modified fly ash mixed with coal, Int. J. Hydrogen Energy 60 (2024) 479–490, https://doi.org/10.1016/j.ijhydene.2024.02.065.

[21] X. Jia, H. Lu, Y. Hui, Y. Zhang, Z. Han, C. Wang, X. Song, G. Xu, Pyrolyzing coal blended with ash: the fate and impacts of CaSO4, J. Anal. Appl. Pyrolysis 169 (2023) 105833, https://doi.org/10.1016/j.jaap.2022.105833.

[22] J. Lai, Y. Meng, Y. Yan, E. Lester, T. Wu, C.H. Pang, Catalytic pyrolysis of linear low-density polyethylene using recycled coal ash: kinetic study and environmental evaluation, Kor. J. Chem. Eng. 38 (2021) 2235–2246, https://doi.org/10.1007/s11814-021-0870-9.

[23] W. Hong, Y. Zhang, H. Jiang, S. Li, J. Chen, L. Zhang, Co-pyrolysis of corn stalk and coal fly ash: a case study on catalytic pyrolysis behavior, bio-oil yield and its characteristics, Case Stud. Therm. Eng. 38 (2022) 102346, https://doi.org/10.1016/j.csite.2022.102346.

[24] R. Wu, P. Lv, B. Liu, Y. Bai, J. Wang, J. Wei, W. Su, G. Xu, W. Bao, G. Yu, Aromatics production from relay catalytic pyrolysis of cow manure using Ru/C and ZSM-5 dual catalysts synthesized from coal gasification fine slag, J. Environ. Manag. 348 (2023) 119356, https://doi.org/10.1016/j.jenvman.2023.119356.

[25] J. de A.O. Marques, J.L.F. Alves, K.F.S. de Oliveira, D.M. de A. Melo, G.A.C. de Melo Viana, R.M. Braga, Catalytic upgrading of pyrolysis vapors from scenedesmus sp. microalgae towards renewable hydrocarbons using a low-cost zeolite synthesized from rice husk ash and diatomite residue, Bioenergy Res. (2024), https://doi.org/10.1007/s12155-024-10732-9.

[26] N. Gao, M. Humphrey Milandile, A. Tariq Sipra, S. Su, N. Miskolczi, C. Quan, Co-pyrolysis of municipal solid waste (MSW) and biomass with Co/sludge fly ash catalyst, Fuel 322 (2022) 124127, https://doi.org/10.1016/j.fuel.2022.124127.

[27] A.S. Al-Rahbi, P.T. Williams, Waste ashes as catalysts for the pyrolysis–catalytic steam reforming of biomass for hydrogen-rich gas production, J. Mater. Cycles Waste Manag. 21 (2019) 1224–1231, https://doi.org/10.1007/s10163-019-00876-8.

[28] K. Lan, S. Shang, C. Guo, T. Xiong, Z. Qin, W. He, J. Li, Preparation of fly ash nickel catalyst and its application in catalytic pyrolysis of rice straw for syngas production, Bioresources 14 (2019) 6983–7000, https://doi.org/10.15376/biores.l4.3.6983-7000.

[29] Y. Li, P.T. Williams, Waste derived ash as catalysts for the pyrolysis-catalytic steam reforming of waste plastics for hydrogen-rich syngas production, J. Anal. Appl. Pyrolysis 177 (2024) 106374, https://doi.org/10.1016/j.jaap.2024.106374.

[30] T. Kobayashi, H. Kuramochi, Catalytic pyrolysis of biomass using fly ash leachate to increase carbon monoxide production and improve biochar properties to accelerate anaerobic digestion, Bioresour. Technol. 387 (2023) 129583, https://doi.org/10.1016/j.biortech.2023.129583.

[31] J. Grafmüller, A. Böhm, Y. Zhuang, S. Spahr, P. Müller, T.N. Otto, T.D. Bucheli, J. Leifeld, R. Giger, M. Tobler, H.-P. Schmidt, N. Dahmen, N. Hagemann, Wood ash as an additive in biomass pyrolysis: effects on biochar yield, properties, and agricultural performance, ACS Sustain. Chem. Eng. (2022), https://doi.org/10.1021/acssuschemeng.1c07694.

[32] J. Song, C. Tang, X. An, Y. Wang, S. Zhou, C. Huang, Catalytic pyrolysis of sawdust with desulfurized fly ash for pyrolysis gas upgrading, Int. J. Environ. Res. Publ. Health 19 (2022), https://doi.org/10.3390/ijerph192315755.

[33] G. Yildiz, F. Ronsse, R. Venderbosch, R. van Duren, S.R.A. Kersten, W. Prins, Effect of biomass ash in catalytic fast pyrolysis of pine wood, Appl. Catal. B Environ. 168–169 (2015) 203–211, https://doi.org/10.1016/j.apcatb.2014.12.044.

[34] F. Guo, K. Peng, T. Li, X. Zhao, Y. Dong, Z. Rao, Catalytic cracking of primary tar vapor from biomass over high ash-containing paper sludge ash, Energy Fuel. 32 (2018) 12514–12522, https://doi.org/10.1021/acs.energyfuels.8b02281.

[35] D. Yao, H. Yang, H. Chen, P.T. Williams, Investigation of nickel-impregnated zeolite catalysts for hydrogen/syngas production from the catalytic reforming of waste polyethylene, Appl. Catal. B Environ. 227 (2018) 477–487, https://doi.org/10.1016/j.apcatb.2018.01.050.

[36] D. Sangaré, S. Bostyn, M. Moscosa Santillán, P. García-Alamilla, V. Belandria, I. Gökalp, Comparative pyrolysis studies of lignocellulosic biomasses: online gas quantification, kinetics triplets, and thermodynamic parameters of the process, Bioresour. Technol. 346 (2022) 126598, https://doi.org/10.1016/j.biortech.2021.126598.

[37] C. Quan, N. Miskolczi, S. Feng, P. Grammelis, C. Wu, N. Gao, Effect of type of activating agent on properties of activated carbon prepared from digested solid waste, J. Environ. Manag. 348 (2023) 119234, https://doi.org/10.1016/j.jenvman.2023.119234.

[38] H. Yang, R. Yan, H. Chen, D.H. Lee, C. Zheng, Characteristics of hemicellulose, cellulose and lignin pyrolysis, Fuel 86 (2007) 1781–1788, https://doi.org/10.1016/j.fuel.2006.12.013.

[39] K. Góra-Marek, M. Derewiński, P. Sarv, J. Datka, IR and NMR studies of mesoporous alumina and related aluminosilicates, Catal. Today 101 (2005) 131–138, https://doi.org/10.1016/j.cattod.2005.01.010.

[40] M.M. Yung, A.K. Starace, M.B. Griffin, J.D. Wells, R.E. Patalano, K.R. Smith, J.A. Schaidle, Restoring ZSM-5 performance for catalytic fast pyrolysis of biomass: effect of regeneration temperature, Catal. Today 323 (2019) 76–85, https://doi.org/10.1016/j.cattod.2018.06.025.

[41] J. Fermoso, H. Hernando, P. Jana, I. Moreno, J. Přech, C. Ochoa-Hernández, P. Pizarro, J.M. Coronado, J. Čejka, D.P. Serrano, Lamellar and pillared ZSM-5 zeolites modified with MgO and ZnO for catalytic fast-pyrolysis of eucalyptus woodchips, Catal. Today 277 (2016) 171–181, https://doi.org/10.1016/j.cattod.2015.12.009.

[42] E.B. Inaloo, M. Saidi, Catalytic pyrolysis of olive pomace for biofuel production: application of metal oxide-modified zeolite catalysts, Biomass Bioenergy 177 (2023) 106947, https://doi.org/10.1016/j.biombioe.2023.106947.

[43] D. Chen, K. Cen, X. Zhuang, Z. Gan, J. Zhou, Y. Zhang, H. Zhang, Insight into biomass pyrolysis mechanism based on cellulose, hemicellulose, and lignin: evolution of volatiles and kinetics, elucidation of reaction pathways, and characterization of gas, biochar and bio-oil, Combust. Flame 242 (2022) 112142, https://doi.org/10.1016/j.combustflame.2022.112142.

[44] D.O. Usino, P. Ylitervo, A. Moreno, M.H. Sipponen, T. Richards, Primary interactions of biomass components during fast pyrolysis, J. Anal. Appl. Pyrolysis 159 (2021), https://doi.org/10.1016/j.jaap.2021.105297.

[45] C.W. Lee, P.Y. Lin, B.H. Chen, R.G. Kukushkin, V.A. Yakovlev, Hydrodeoxygenation of palmitic acid over zeolite-supported nickel catalysts, Catal. Today 379 (2021) 124–131, https://doi.org/10.1016/j.cattod.2020.05.013.

[46] G. Yildiz, T. Lathouwers, H.E. Toraman, K.M. Van Geem, G.B. Marin, F. Ronsse, R. Van Duren, S.R.A. Kersten, W. Prins, Catalytic fast pyrolysis of pine wood: effect of successive catalyst regeneration, Energy Fuel. 28 (2014) 4560–4572, https://doi.org/10.1021/ef500636c.

[47] D.K. Ratnasari, W. Yang, P.G. Jönsson, Catalytic pyrolysis of lignocellulosic biomass: the influence of the catalyst regeneration sequence on the composition of upgraded pyrolysis oils over a H-ZSM-5/Al-MCM-41 catalyst mixture, ACS Omega 5 (2020) 28992–29001, https://doi.org/10.1021/acsomega.0c03272.

[48] M. Hoseini, F. Atashi, M. Gholizadeh, F. Clarens, Coke Formation and zeolite catalyst effects on products from Co-pyrolysis of waste tyre and poplar wood in a semi-batch reactor under N2 atmosphere, Energy Technol. 12 (2024) 2300740, https://doi.org/10.1002/ente.202300740.

[49] M. do C. Rangel, F.M. Mayer, M. da S. Carvalho, G. Saboia, A.M. de Andrade, Selecting catalysts for pyrolysis of lignocellulosic biomass, Biomass 3 (2023) 31–63, https://doi.org/10.3390/biomass3010003.

[50] A.N. Shafawi, A.R. Mohamed, P. Lahijani, M. Mohammadi, Recent advances in developing engineered biochar for CO2 capture: an insight into the biochar modification approaches, J. Environ. Chem. Eng. 9 (2021) 106869, https://doi.org/10.1016/j.jece.2021.106869.

[51] M. Artetxe, G. Lopez, M. Amutio, G. Elordi, J. Bilbao, M. Olazar, Cracking of high density polyethylene pyrolysis waxes on HZSM-5 catalysts of different acidity, Ind. Eng. Chem. Res. 52 (2013) 10637–10645, https://doi.org/10.1021/ie4014869.

[52] Y. Li, Nishu, D. Yellezuome, C. Li, R. Liu, Deactivation mechanism and regeneration effect of bi-metallic Fe-Ni/ZSM-5 catalyst during biomass catalytic pyrolysis, Fuel 312 (2022) 122924, https://doi.org/10.1016/j.fuel.2021.122924.

[53] V. Daligaux, R. Richard, M. Marin-Gallego, V. Ruaux, L. Pinard, M.H. Manero, Deactivation by coking of industrial ZSM-5 catalysts used in LDPE pyrolysis and regeneration by ozonation process – bench scale studies, Appl. Catal. Gen. 671 (2024) 119581, https://doi.org/10.1016/j.apcata.2024.119581.

[54] A. Ochoa, J. Bilbao, A.G. Gayubo, P. Castaño, Coke formation and deactivation during catalytic reforming of biomass and waste pyrolysis products: a review, Renew. Sustain. Energy Rev. 119 (2020) 109600, https://doi.org/10.1016/j.rser.2019.109600.

[55] X. Deng, J. Deng, R. He, X. Xie, Y. Xu, S. Yuan, Effects of Ba and Mg promoters on gas release from Fe catalyzed coal pyrolysis: effects of different precursors, Fuel 308 (2022), https://doi.org/10.1016/j.fuel.2021.121977.

[56] W. Liu, M. Song, X. Wang, C. Wang, C. Zhang, Study on the synergistic effect

between Ni and Me species over Ni-Me/HZSM-5 on the in-situ catalytic pyrolysis of alkali lignin, Appl. Catal. Gen. 663 (2023) 119270, https://doi.org/10.1016/j.apcata.2023.119270.

[57] N. Guilhaume, Y. Schuurman, C. Geantet, The role of catalysis in the valorization of woody biomass fast pyrolysis liquids: overview and contribution of IRCELYON, Catal. Today 373 (2021) 5–23, https://doi.org/10.1016/j.cattod.2021.03.030.